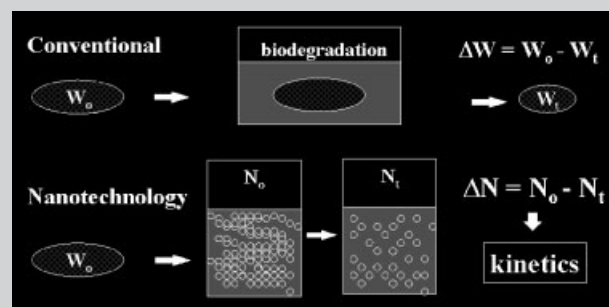


Summary: The microphase inversion of water-insoluble poly(L-lactide), “poly[(L-lactide)-*co*-glycolide] and polylactide-*block*-poly(ethylene oxide)-*block*-polylactide from THF to water can result in narrowly distributed stable particles. Gliclazide, a commercial drug, can be encapsulated inside during the process. The formation and degradation of such particles was studied by laser light scattering. In comparison with the corrosion of a bulk material, the degradation of each particle is so fast that we only detect the decrease of the particle number, not the corrosion of individual particles. Therefore, the degradation is a “one-by-one” random process, just like the chemical reaction of molecules in solution. The disappearing rate of the particle number is nearly independent of time, ideal for the controlled release of drugs encapsulated inside. The amount of encapsulated gliclazide depends on the copolymer’s hydrophobicity (composition), while the releasing rate mainly is, directly related to the

disappearing rate of the particles. The correlation between the fluorescence intensity and the degradation was used to study the kinetics of gliclazide releasing. The releasing pattern is controllable with a proper choice of the drug loading, copolymer composition, pH and temperature.



Erosion Induced Controllable Release of Gliclazide Encapsulated Inside Degradable Polymeric Particles

Yue Zhao,^{1,2} Wenna Chen,² Qing Cai,² Shenguo Wang,² Jun Bo,³ Chi Wu*^{1,4}

¹The Open Laboratory of Bond-selective Chemistry, Department of Chemical Physics, University of Science and Technology of China, Hefei, Anhui, China, 230026

Fax: 0086 852 2603 5057; E-mail: chiwu@cuhk.edu.hk

²State Key Laboratory of Polymer Physics and Chemistry, Institute of Chemistry, Chinese Academy of Science, Beijing 100080, P. R. China

³Anhui Medical Institute, Hefei, Anhui, China, 230000

⁴Department of Chemistry, The Chinese University of Hong Kong, Shatin, N.T., Hong Kong

Received: October 2, 2003; Revised: January 12, 2004; Accepted: January 16, 2004; DOI: 10.1002/mabi.200300061

Keywords: colloids; controllable drug releasing; light scattering; micronization; polyesters

Introduction

Biocompatible and biodegradable polymers have many potential biomedical applications, such as surgical sutures, orthopedic implants, scaffolds for cells in tissue engineering and controllable drug releasing devices.^[1–5] They have recently attracted much attention. Aliphatic polyesters, e.g., poly(lactic acid) (PLA), poly(glycolic acid) (PGA) and poly(ϵ -caprolactone) (PCL) and their copolymers derivatives are often used because of their tested biocompatibility and non-toxicity.^[6–9] The biodegradation of these polyesters often leads to pharmacologically inactive substances such as lactic acid from PLA and 6-hydroxycaproic acid from PCL, which are absorbable by the body or removable by metabolism.^[10,11] Therefore, biodegradable aliphatic polyesters have a distinct advantage over other types of

biomedical materials because it is not necessary to remove them with a second surgical operation.

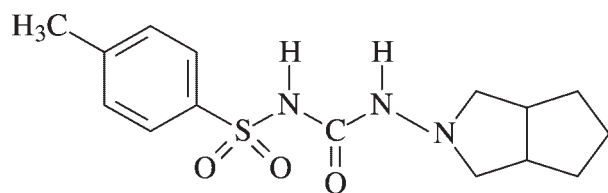
In the past, we used the microphase inversion to prepare polymeric nanoparticles^[9,12] and studied the formation and structure of resultant nanoparticles by a combination of static and dynamic laser light scattering.^[13] For biodegradable polymers, we found that the degradation rate of these nanoparticles is nearly constant for a given set of experimental conditions,^[9,12] ideal for the controllable release of drugs. It is helpful to note that the degradation of these nanoparticles in dispersion is different from that of a bulk material – the corrosion of a bulk material is like the layer-by-layer peel of an onion, but the degradation of each nanoparticle is so fast that we only observe the decrease of the particle number, not the particle size.^[9,12] Our previous studies showed that the degradation of these nanoparticles

is a random “one-by-one”, not “none-or-all” process.^[9,12] On the basis of the previous studies, we decided to use these biodegradable nanoparticles to encapsulate drugs and investigate whether their degradation can be really used to release drugs in a controllable fashion for biomedical applications.

In this study, gliclazide was chosen as a testing drug. It is a second generation of hypoglycemic sulfonylureas,^[14] a useful drug for a long-term treatment of non-insulin-dependent diabetic mellitus (NIDDM) because of its good general tolerance, low incidence of hypoglycemia^[15,16] and a low rate of secondary failure.^[17] Its chemical structure is shown in Scheme 1.

Normally, a rapid gastrointestinal adsorption is required for oral hypoglycemic drugs. However, the absorption rate of gliclazide is rather slow, a major drawback in the application of gliclazide in the form of oral dosage. It is generally attributed to its poor solubility in water because of its hydrophobic nature. The enhancement of its solubility in aqueous solution is one way of accelerating its gastrointestinal absorption.^[18,19]

In the present study, by using biodegradable and biocompatible polymeric nanoparticles to encapsulate gliclazide, we are able to greatly enhance its solubility in water and also to control its releasing rate. It has generally been known that polymeric nanoparticles can be made into various dosage forms, including intravenous and oral routes to increase the bio-availability and reduce the associated adverse effects.^[20–23] Narrowly distributed stable polymeric nanoparticles are ideal for intravenous injection because they can easily pass through the blood vessels.^[24] It has even been suggested that by a proper regulation of the particle size, one could target different organs. It should be noted that many pharmaceutical studies of using such polymers have been conducted and the main focus is on the development of controllable releasing implants entrapped with active ingredients.^[25,26] The possibilities of using nanoparticles for such a purpose have also been explored^[27–30] but the encapsulation of a high content of active ingredient inside the nanoparticles is far more difficult in comparison with a bulk material. Using the microphase inversion, we re-dispersed three different water-insoluble polymers, poly(lactide) (PLA) homopolymer, poly[(L-lactide)-*co*-glycolide] (PLG) random copolymer and poly(lactide)-*block*-poly(ethylene oxide)-*block*-poly(lactide) (PLE) triblock copolymer into stable



Scheme 1.

nanoparticles in water with and without the help of surfactants. During the inversion process, gliclazide can be entrapped inside the resultant particles. In this way, the dissolution of gliclazide in water is enhanced and the releasing rate of gliclazide on the basis of the corrosion of these particles is controllable.

Experimental Part

Sample Preparation

Poly(L-lactide) (PLA), poly[(L-lactide)-*co*-glycolide] (PLG) random copolymer with different composition were synthesized by homopolymerization or copolymerization of a prescribed amount of L-lactide (LA) (Shanghai Yierbao Lactide Acid Products Manufacture) with glycolide (GA) (Beijing Xizhong Chemical Plant) with ethylene glycol at 140 °C for ≈24 h. poly(lactide)-*block*-poly(ethylene oxide)-*block*-poly(lactide) (PLE) triblock copolymer was synthesized by copolymerization of a prescribed amount of L-lactide with poly(ethylene glycol) ($\bar{M}_w = 10^4$ g/mol) (Tianjin Eastern Health Materials Factory) at 140 °C with stannous octoate (Aldrich Chemical Company) as a catalyst for 30 h. Gliclazide is from the Anhui Medical Institute, Hefei, Anhui, China. The synthetic details can be found elsewhere.^[31,32] The molar ratio of LA to GA calculated from ¹H NMR spectrum and the weight-average molar mass (\bar{M}_w), determined from GPC by using polystyrenes as standard, of the polymers used are listed in Table 1.

PLA, PLG, PLE and gliclazide are soluble in tetrahydrofuran (THF). The PLA and PLG particles were prepared by adding 1.0 mL dilute solution mixture of gliclazide and the polymer in THF dropwise into 100 mL water in the presence of cationic surfactant hexadecyltrimethylammonium bromide (HTAB). The surfactant concentration was kept at one critical micelle concentration ($\text{CMC} \approx 3.3 \times 10^{-4}$ g/mL). As expected, solvent THF mixes with water as soon as the solution is dropped in. At the same time, hydrophobic polymer chains undergo intrachain contraction and interchain association, i.e., the microphase inversion. The interchain aggregations are quickly stabilized by cationic surfactant adsorbed on their surface to form stable nanoparticles. During the process, water-insoluble gliclazide is entrapped inside the hydrophobic particles. The small amount of THF (1%) introduced in the process was removed under reduced pressure, which has no effect on the size and stability of such formed particles. The pH of the dispersion was adjusted by sodium hydroxide (NaOH)

Table 1. Characterizations of poly(lactide) (PLA), poly(lactide)-*co*-glycolide) (PLG) and poly(lactide)-*block*-poly(ethylene oxide)-*block*-poly(lactide) (PLE) by NMR and GPC.

Sample	PLA	PLG9505	PLG9010	PLE
LA/GA/EG (feeding mol ratio)	100/0/0	95/5/0	90/10/0	80/0/20
\bar{M}_w	149 000	146 000	121 000	112 000
\bar{M}_w/\bar{M}_n	2.12	1.87	2.21	1.83

aqueous solution. PLE can be similarly micronized without the help of cationic surfactant.

The resultant aqueous dispersion was stored at the room temperature for two days before it was clarified with a 1.2 μm filter to remove small amount of precipitates (a mixture of polymer and gliclazide). In this way, the first pulse of gliclazide in the releasing study was avoided. The solubility of gliclazide powder in distilled water at the room temperature is 1.5 $\mu\text{g}/\text{mL}$, determined by UV-visible spectrophotometer (CARY 50 Conc) at 227 nm after re-dissolving proper amount of dried gliclazide aqueous solution in THF. The fluorescence emission was recorded by spectrofluorometer (CARY Eclipse). The excitation wavelength used in the fluorescence measurement was 264 nm and the exiting slit width was 5 nm. The beam path used in both the spectrometers was 1.0 cm.

Laser Light-Scattering (LLS)

A modified commercial LLS spectrometer (ALV/SP-125) equipped with an ALV-5000 multi- τ digital time correlator and a solid state laser (DPSS, ≈ 400 mV at $\lambda = 532$ nm) was used. In static LLS, the angular and concentration dependence of the excess absolute time-average scattered intensity, i.e. Rayleigh ratio $R_{\text{VV}}(q)$ of a dilute dispersion can lead to the weight-average molar mass \bar{M}_w , the second virial coefficient A_2 , and the root-mean square z-average radius $\langle R_g^2 \rangle_z^{1/2}$ (or simply as $\langle R_g \rangle$)^[33], i.e.,

$$\frac{KC}{R_{\text{VV}}(q)} = \frac{1}{\bar{M}_w} \left(1 + \frac{1}{3} \langle R_g^2 \rangle_z q^2 \right) + 2A_2C \quad (1)$$

where q is the scattering vector. In dynamic LLS, the Laplace inversion of a measured intensity-intensity time correlation function $G^{(2)}(t, q)$ in the self-beating mode can lead to a line-width distribution $G(\Gamma)$.^[23,24] For a pure diffusive relaxation, $(\Gamma/q^2)_{q \rightarrow 0, c \rightarrow 0}$ leads to the translational diffusion coefficient D or further to the hydrodynamic radius R_h via the Stokes-Einstein equation. The dispersion was clarified by 0.8 μm Millipore filter to remove dust. The sodium hydroxide (NaOH) aqueous solution for the adjustment of pH was clarified by 0.1 μm Millipore filter. In a typical degradation experiment, a proper amount of dust-free NaOH aqueous solution was in situ added into 2 mL dust-free dispersion. Both $R_{\text{VV}}(q)$ and $G^{(2)}(t, q)$ were simultaneously measured during the degradation. The details of LLS theory and instrumentation can be found elsewhere.^[33–35]

Results and Discussion

Figure 1 shows typical hydrodynamic radius distributions of resultant PLA, PLG and PLE nanoparticles with gliclazide encapsulated inside, where $f(R_h)$ s were measured in dynamic LLS. No interparticles aggregation in water was observed over a long time. The average hydrodynamic radius $\langle R_h \rangle$ calculated from $\int f(R_h)R_h dR_h$ is in the range 180–245 nm. Table 2 summarizes the measured average hydrodynamic radii of the PLA, PLG and PLE nanoparticles in water. They are narrowly distributed with a relative

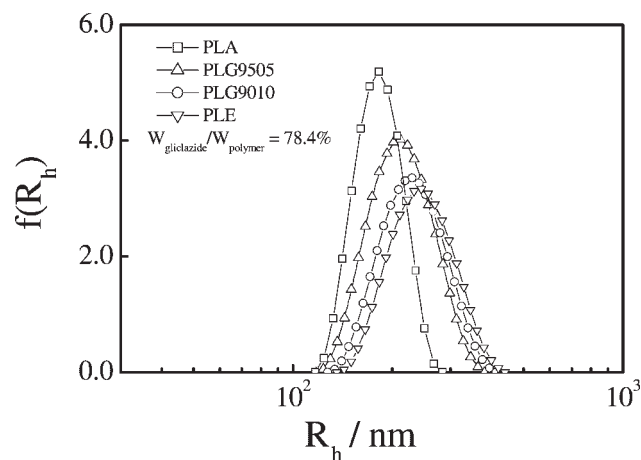


Figure 1. Typical hydrodynamic radius distributions $f(R_h)$ of PLA, PLG9505, PLG9010 and PLE nanoparticles with gliclazide encapsulated inside in de-ionized water, where $T = 25$ °C, $\text{pH} = 6.3$, and $C_{\text{polymer}} = 3.34 \times 10^{-5}$ g/mL.

line width $(\mu_2/\langle R_h \rangle^2)$ of not more than 0.2 where μ_2 is defined as $\int (R_h - \langle R_h \rangle)^2 f(R_h) dR_h / \langle R_h \rangle^2$. Table 2 also shows that the loading of different amounts of gliclazide has less effect on the particle size. On the other hand, the particle size increases with the polymer hydrophilicity. This is reasonable because of the swelling of hydrophilic polymer chains in water.^[36]

Figure 2 shows typical fluorescence emission spectra of gliclazide in water. The peaks at 288 nm and 577 nm are typical fluorescence signals for gliclazide. Since the peak at 288 nm is mixed with the signal from the polymer, we therefore used the peak at 577 nm to estimate the amount of gliclazide in the solution. The inset shows that the area of the fluorescence peak located at 577 nm increases with the feeding gliclazide content. The theoretical line is calculated by assuming that all gliclazide molecules were entrapped inside the nanoparticles. Using this line as a reference, we can determine the actual amount of gliclazide entrapped inside the resultant polymeric particles.

Figure 3 shows that the presence of polymeric particles clearly increases the solubility of gliclazide in water. Note that the solubility of gliclazide in pure water is only 1.5 $\mu\text{g}/\text{mL}$. It is clear that all the polymers used can enhance the

Table 2. Laser light-scattering characterization of PLA, PLG and PLE nanoparticles with gliclazide encapsulated inside where $T = 25$ °C and $\text{pH} = 6.3$.

$W_{\text{gliclazide}}/W_{\text{polymer}}$ (%)	78.4	70.8	54.8	32.6
$\langle R_h \rangle_{\text{PLA}}^a/\text{nm}$	185	189	182	190
$\langle R_h \rangle_{\text{PLG9505}}/\text{nm}$	230	212	224	245
$\langle R_h \rangle_{\text{PLG9010}}/\text{nm}$	237	214	225	186
$\langle R_h \rangle_{\text{PLE}}/\text{nm}$	245	234	232	220

^{a)} Relative errors: $\langle R_h \rangle \pm 2\%$.

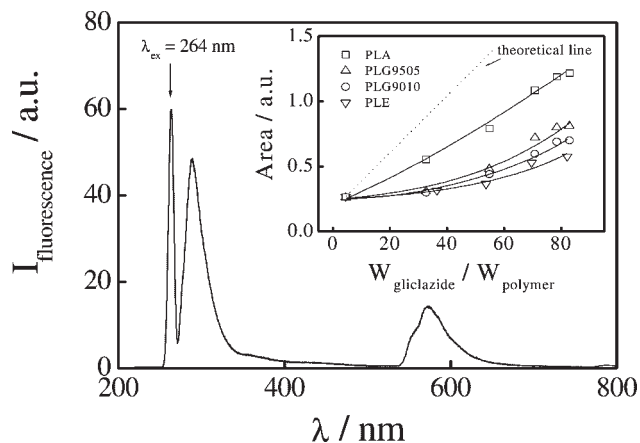


Figure 2. Typical fluorescence emission spectrum of a gliclazide saturated aqueous solution where the excited wavelength is 264 nm. The inset shows the feeding gliclazide-to-polymer weight ratio dependence of the area under the fluorescence peak located at 577 nm, where C_{polymer} is kept at 3.34×10^{-5} g/mL.

dissolution of gliclazide in water and the solubility increases with the loading of gliclazide. It is interesting to find that the efficiency of encapsulating gliclazide increases with the PLA content. It has been reported that the polymer-gliclazide interaction is critical in controlling the drug releasing characteristics.^[37–39] Our results show that the encapsulation of gliclazide inside the particles is mainly determined by hydrophobic interaction. For the triblock copolymer, the collapsed hydrophobic PLE core is stabilized by the swollen hydrophilic shell made of short hydrophilic PEO chains. It explains why such “core-shell” particles encapsulate the least amount of gliclazide. Therefore, the drug loading inside the nanoparticles can be controlled by varying either the polymer hydrophilicity (composition) or the feeding gliclazide-to-polymer weight

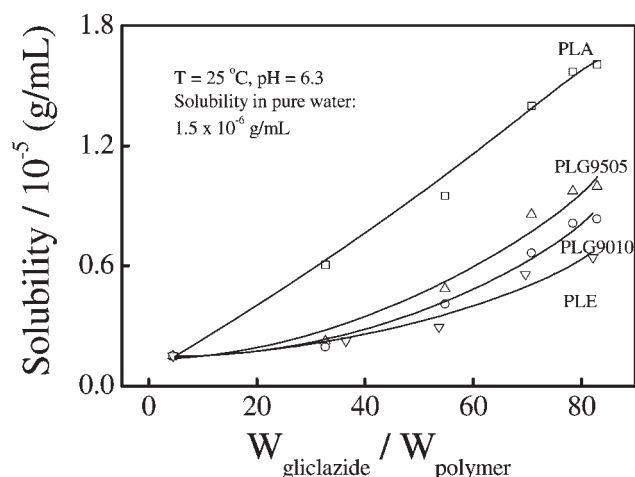


Figure 3. Feeding gliclazide-to-polymer weight ratio dependence of solubility of gliclazide in water. The solubility of gliclazide in pure water without polymeric particles is only 1.5 $\mu\text{g/mL}$.

ratio in THF solution. The latter is easier and cheaper, but there exists a maximum loading for each given copolymer. It is helpful to note that the degradation of the particles at $\text{pH} = 6.3$ is extremely slow. In order to promote the degradation and study it over a reasonable time period so that the measurement can be properly done, we increase the pH value to speed up the hydrolysis.

Figure 4 shows that the fluorescence intensity decreases with an increasing degradation time at $\text{pH} = 10.4$. It has been stated before that the fluorescence peak at 577 nm is related to gliclazide. Note that the fluorescence intensity has nearly no change during the degradation of pure PLA nanoparticles. The decrease of the fluorescence intensity must be due to the release of gliclazide originally entrapped inside the nanoparticles. It is helpful to note that without the protection of the nanoparticles, the released gliclazide is insoluble and precipitates out of the dispersion. Therefore, it has no contribution in the fluorescence intensity. From the decrease of the peak area, we can estimate the releasing rate of gliclazide. The inset of Figure 4 shows the decrease of the relative Rayleigh ratio ($R_{\text{vv}}(q)_t / R_{\text{vv}}(q)_0$) during the degradation, where $R_{\text{vv}}(q)$ is proportional to the scattering intensity measured in static LLS. Equation (1) shows that $R_{\text{vv}}(q)$ is proportional to NM^2 , where N and M are the number and mass of the particles, respectively. Dynamic LLS results showed that there was no change in the size of the remaining particles, i.e., no change in M during the degradation. Therefore, the decrease of $R_{\text{vv}}(q)$ must be directly related to the particle number N . It has been known that the degradation is not a “none-or-all” process, but proceeds in a random “one-by-one” fashion.^[9,12] A combination of LLS and fluorescence shows that gliclazide is released as soon as the degradation starts. Taking the initial peak area (A_0) as a reference, we can study the releasing kinetics of gliclazide by calculating the relative extent

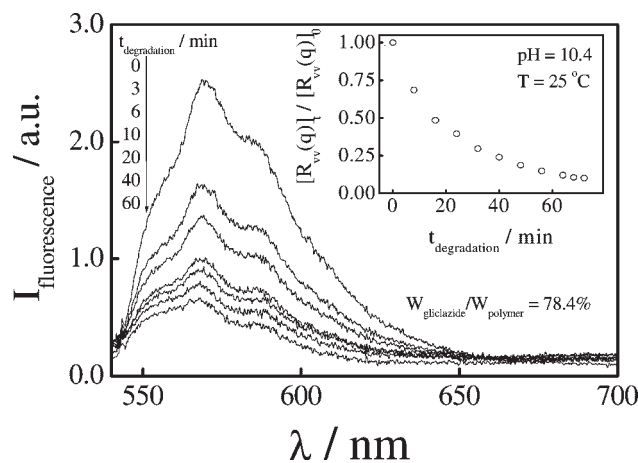


Figure 4. Degradation time dependence of fluorescence intensity of PLA nanoparticles with gliclazide encapsulated inside, where $C_{\text{polymer}} = 3.34 \times 10^{-5}$ g/mL. The inset shows the degradation time dependence of the relative Rayleigh ratio ($R_{\text{vv}}(q)_t / R_{\text{vv}}(q)_0$) measured in static laser light scattering.

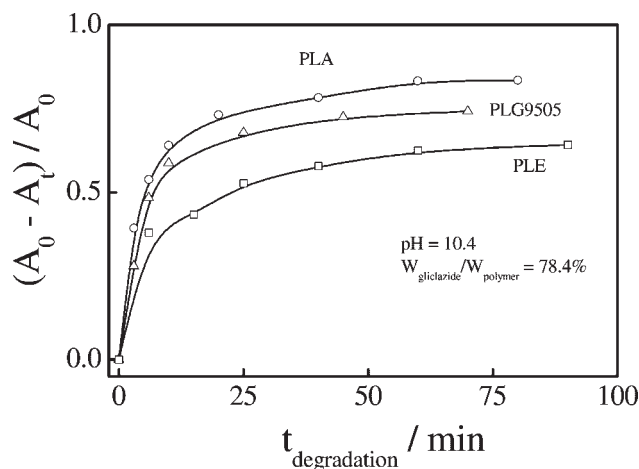


Figure 5. Releasing pattern of gliclazide from PLA, PLG9505 and PLE nanoparticles in terms of the relative change of the fluorescence peak area located at 577 nm, where the subscript “0” and “t” represent to the peak area at time 0 and t , respectively, where $C_{\text{polymer}} = 3.34 \times 10^{-5}$ g/mL.

of the release $[(A_0 - A_t)/A_0]$ versus the degradation time ($t_{\text{degradation}}$).

Figure 5 shows that both the initial releasing rate and the final releasing extent increase with the copolymer PLA content. This can be explained as follows. As the degradation proceeds, both PLA and PLG are decomposed into different low molar mass acids, which neutralize OH^- so that pH decreases and further hydrolysis is suppressed. It is helpful to note that resultant glycolic acid (GA) is more acidic than lactic acid (LA). Therefore, the suppressing effect is stronger in the case of PLG nanoparticles. This is why we observed a slower releasing rate of gliclazide when PLG was used. The PLE particles have the slowest releasing rate because poly(ethylene oxide) (PEO) chains, the degradation product of PLE, act as co-solvent to stabilize some of gliclazide molecules in water^[18] preventing their precipitation in water and leading to apparent slower releasing rate. Figure 5 clearly demonstrates that a desirable releasing pattern can be obtained by a proper choice of the copolymer composition.

Figure 6 shows that loading different amounts of gliclazide into the nanoparticles have no effect on the relative releasing rate. It indicates that gliclazide released in such a system mainly depends on the degradation of the nanoparticles and the loading extent does not effect on the releasing kinetics. Our previous studies showed that the degradation of individual nanoparticles is extremely fast and the degradation follows a random “one-by-one” process. Therefore, the drug is released after the degradation of each nanoparticle. This also explains why different loading extents of gliclazide have the same relative releasing pattern. However, it should be noted that the absolute releasing rate is proportional to the average amount of gliclazide encapsulated inside each nanoparticle. Therefore, we can

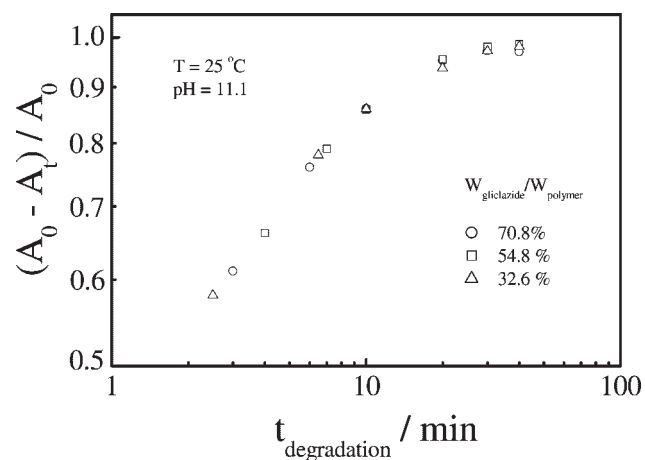


Figure 6. Releasing pattern of gliclazide from PLA nanoparticles with different initial feeding gliclazide-to-polymer weight ratios.

regulate the amount of gliclazide released per unit time by changing the drug loading extent. This is very useful in real applications.

Figure 7 shows that both the initial releasing rate and final relative releasing extent increase with pH. This is due to the higher hydrolysis rate of the polymer chain backbones at higher pH values. Adjusting the pH value, we can vary the releasing rate from minutes to days. Such a pH dependent degradation should be useful in the pH-regulated controllable releasing application. It is helpful to note that the releasing rate is extremely slow when pH is lower than 9. This is particularly important because each polymeric nanoparticle can act as a protective matrix to carry drugs through stomach (acidic environment) and release them in intestines in a controllable fashion because in the process pH increases from ≈ 3 to 10–11. Applications of these polymeric particles in this direction are being investigated.

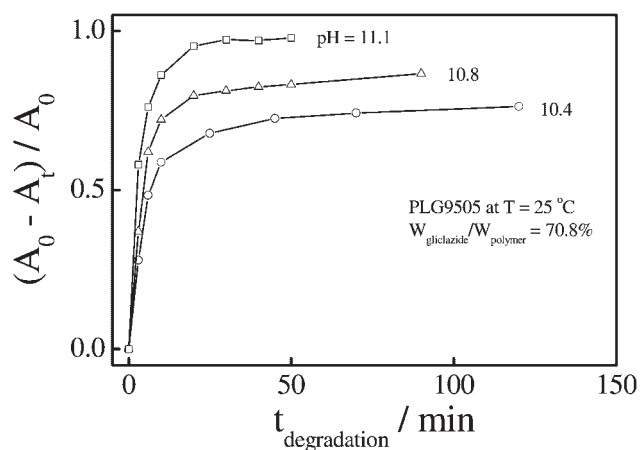


Figure 7. pH dependence of releasing pattern of gliclazide from PLG9505 nanoparticles, where $C_{\text{polymer}} = 3.34 \times 10^{-5}$ g/mL.

Conclusions

Water-insoluble poly(L-Lactide) (PLA) homopolymer, poly[(L-lactide)-*co*-glycolide] (PLG) random copolymer and polylactide-*block*-poly(ethylene oxide)-*block*-polylactide (PLE) triblock copolymer can be re-dispersed into narrowly distributed nanoparticles stable in water via microphase inversion with and without the help of surfactant. During the process, gliclazide, a second generation of hypoglycemic sulfonylureas, can be conveniently entrapped inside. Such a formulation greatly enhances the drug's solubility in water and its bio-availability. The relative releasing rate of gliclazide is mainly controlled by the particle degradation rate. The average amount of gliclazide loaded inside each nanoparticle can be regulated by a variation of the polymer hydrophobicity (composition) as well as the initial feeding gliclazide-to-polymer weight ratio, which leads to a control of the amount of gliclazide released per unit time. It should be mentioned once more that the releasing mechanism used in this study is different from the corrosion or diffusion-induced release of drugs from a bulk material. If a bulk drug carrier is used, a gradient loading of drugs from center to periphery is essential to ensure a constant releasing rate. It is not easy to realize and control such a gradient drug loading in practice. In the case of using small polymeric nanoparticles, the releasing rate is related to a "one-by-one" random degradation of individual particles and the degradation of each particle is so fast that no gradient loading is required. The method demonstrated in the present study should make the formulation much easier.

Acknowledgement: The financial support of the CAS Bai Ren Project, the China NNSF Project 2002/03 (20274045) and the HKSAR Earmarked RGC Grants (CUHK4025/02P, 2160181) is gratefully acknowledged.

- [1] L. B. Peppas, *Int. J. Pharm.* **1995**, *116*, 1.
- [2] R. Langer, *Science* **1990**, *249*, 1527.
- [3] R. Langer, J. Vacanti, *Science* **1993**, *260*, 920.
- [4] R. Chandra, R. Rustgi, *Prog. Polym. Sci.* **1998**, *23*, 1273.
- [5] S. S. Davis, *J. Pharm. Pharmacol.* **1992**, *51*, 186.
- [6] I. Engelberg, J. Kohn, *Biomaterials* **1991**, *12*, 292.
- [7] A. Albertsson, S. Karlsson, *Acta. Polym.* **1995**, *46*, 114.
- [8] H. Fessi, F. Puisieux, J. P. Devissaguet, S. Benita, *Int. J. Pharm.* **1989**, *55*, R1.
- [9] Z. Gan, T. F. Jim, M. Li, Y. Zhao, S. G. Wang, C. Wu, *Macromolecules* **1999**, *32*, 590.
- [10] R. Lenz, *Adv. Polym. Sci.* **1993**, *107*, 3.
- [11] H. Shibayama, H. Yasuda, Y. Doi, K. Fukuda, "Biodegradable Plastics and Polymers", Elsevier, Amsterdam 1994, p. 541.
- [12] Y. Zhao, T. J. Hu, Z. Lv, S. G. Wang, C. Wu, *J. Polym. Sci., Part B: Polym. Phys.* **1999**, *37*, 3288.
- [13] Y. Zhao, H. J. Liang, S. G. Wang, C. Wu, *J. Phys. Chem., Part B* **2001**, *105*, 848.
- [14] L. P. Krall, *Diabetes Res. Clin. Pract.* **1991**, *14*, S15.
- [15] K. L. Palmer, R. N. Brogden, *Drugs* **1993**, *46*, 92.
- [16] J. Mailhot, *Clin. Ther.* **1993**, *15*, 1060.
- [17] A. D. Harrower, *J. Diabetes Complications* **1994**, *8*, 201.
- [18] S. S. Hong, S. H. Lee, Y. J. Lee, S. J. Chung, M. H. Lee, C. K. Shim, *J. Control. Release* **1998**, *51*, 185.
- [19] Y. Ozkan, T. Atay, N. Dikmen, A. Isimer, H. Y. Aboul-Enein, *Pharm. Acta Helvetica* **2000**, *74*, 365.
- [20] K. S. Soppimath, T. M. Aminabhavi, A. R. Kulkarni, W. E. Rudzinski, *J. Controlled Release* **2001**, *70*, 1.
- [21] P. Maincent, V. R. Le, P. Sado, P. Couvreur, J. Devissaguet, *J. Pharm. Sci.* **1986**, *75*, 955.
- [22] P. Couvreur, L. Grislain, V. Lenaerts, P. Brasseur, P. Guiot, A. Biernacki, in: "Polymeric Nanoparticles and Microspheres", P. Guiot, P. Couvreur, Eds., CRC Press, Boca Raton 1986, p. 27.
- [23] K. Little, J. Parkhouse, *Lancet* **1962**, *2*, 857.
- [24] G. Thews, E. Mutschler, P. Vaupel, "Anatomie, Physiologie, Pathophysiologie des Menschen", Wissenschaftl. Verlagsges, Stuttgart 1980, p. 229.
- [25] A. Gopferich, M. J. Alonso, R. Langer, *Pharm. Res.* **1994**, *11*, 1568.
- [26] P. G. Jenkins, K. A. Howard, N. W. Blackhall, N. M. Thomas, S. S. Davis, D. T. O'Hagan, *J. Controlled Release* **1994**, *29*, 339.
- [27] E. Allemann, R. Gurny, B. Doelker, F. S. Skinner, H. Schiitz, *J. Controlled Release* **1994**, *29*, 97.
- [28] R. Gref, Y. Minamitake, M. T. Peracchia, V. Trubetskoy, V. Torchilin, R. Langer, *Science* **1994**, *263*, 1600.
- [29] A. Belbella, C. Vauthier, H. Fessi, J. P. Devissaguet, F. Puisieux, *Int. J. Pharm.* **1996**, *129*, 95.
- [30] M. D. Coffin, J. M. McGinity, *Pharm. Res.* **1992**, *9*, 200–205.
- [31] Q. Cai, J. Z. Bei, S. G. Wang, *J. Biomater. Sci., Polym. Ed.* **2000**, *11*, 273.
- [32] Q. Cai, J. Z. Bei, S. G. Wang, *Polym. Adv. Technol.* **2000**, *11*, 159.
- [33] B. Chu, "Laser Light Scattering", 2nd edition, Academic Press, New York 1991.
- [34] B. Berne, R. Pecora, "Dynamic Light Scattering", Plenum Press, New York 1976.
- [35] C. Wu, S. Q. Zhou, *Macromolecules* **1995**, *28*, 8381.
- [36] D. R. Chen, H. L. Chen, J. Z. Bei, S. G. Wang, *Polym. Int.* **2000**, *49*, 269.
- [37] S. Li, S. G. Holland, M. Vert, *J. Control. Release* **1996**, *40*, 41.
- [38] H. Okada, Y. Doken, Y. Ogawa, H. Toguchi, *Pharm. Res.* **1994**, *11*, 1143.
- [39] M. Miyajima, A. Koshika, J. Okada, M. Ikeda, *J. Control. Release* **1999**, *61*, 295.